OncoTargets and Therapy

Dovepress
open access to scientific and medical research

Open Access Full Text Article

ORIGINAL RESEARCH

IL-21-secreting hUCMSCs combined with miR-200c inhibit tumor growth and metastasis via repression of Wnt/β-catenin signaling and epithelial–mesenchymal transition in epithelial ovarian cancer

This article was published in the following Dove Press journal:
OncoTargets and Therapy

Yunxia Zhang[1,2]
Jing Wang[2]
Di Wu[1]
Miao Li[1]
Fenshu Zhao[1]
Mulan Ren[2]
Yunlong Cai[2]
Jun Dou[1]

[1]Department of Pathogenic Biology and Immunology, School of Medicine, Southeast University, Nanjing, People's Republic of China; [2]Department of Gynecology & Obstetrics, Zhongda Hospital, School of Medicine, Southeast University, Nanjing, People's Republic of China

Background: Epithelial ovarian cancer (EOC) with insidious characteristic manifests no symptoms in its early onset but most patients have advanced and distant cancer metastasis at diagnosis. Innovative early diagnosis and effective treatment of EOC are urgently needed.

Methods: In the study, we developed a novel agent of IL-21-secreting human umbilical cord mesenchymal stem cells (hUCMSCs) combined with miR-200c to evaluate its effects on SKOV3 EOC in vitro and in vivo.

Results: hUCMSCs-LV-IL-21 combined with miR-200c significantly inhibited the SKOV3 cell mobility and tumorigenesis compared with hUCMSCs-LV-IL-21, hUCMSCs- LV-vector, and hUCMSCs, respectively. These were reflected in decreasing the tumor sizes and elongating the tumor bearing nude mouse survival, accompanied with increasing the serum cytokine levels of IFN-γ, IL-21 and TNF-α as well as the splenocyte cytotoxicity. In addition, the expression of β-catenin, cyclin-D1, Gli1, Gli2, and ZEB1 was decreased but the E-cadherin expression was increased in tumor tissues of mice treated with hUCMSCs-LV-IL-21 plus miR-200c.

Conclusion: We demonstrated that the synergistic effect of fighting SKOV3 EOC is attributable to repression of Wnt/β-catenin signaling and epithelial-mesenchymal transition in SKOV3 EOC. The findings may provide a new strategy for therapy of EOC.

Keywords: epithelial ovarian cancer, umbilical cord mesenchymal stem cells, IL-21, miR-200c, Wnt/β-catenin signaling, epithelial–mesenchymal transition

Introduction

Epithelial ovarian cancer (EOC) is the most lethal gynecological malignancy. In more than half EOC patients, the disease has already progressed by the time they are diagnosed, so it has been considered as a "silent killer." Although the treatment with platinum and taxanes is initially effective in 80% of EOC patients, uncontrolled metastases still account for the most patient deaths. So far, the standard treatment of ovarian cancer is surgical treatment in combination with platinum-based chemotherapy; however, chemoresistance has been an insurmountable problem. As such, there is an unmet need for finding a new treatment method to increase the therapeutic effect on EOC patients.[1–3]

Recent advances have highlighted the potential of immunotherapeutic approaches for ovarian cancer. Cytokine treatment remains a primary modality of tumor immunotherapy

Correspondence: Jun Dou
Department of Pathogenic Biology and Immunology, Medical School, Southeast University, Nanjing 210009, People's Republic of China
Tel +86 25 8327 2454
Fax +86 25 8332 4887
Email njdoujun@seu.edu.cn

submit your manuscript | www.dovepress.com
Dovepress
http://dx.doi.org/10.2147/OTT.S147855

by activating immune cells in vivo.[4,5] Due to their capacity to regulate cellular and humoral immunity, cytokines are increasingly used as gene therapy for treatment of tumors by systemic injection. Interleukin (IL)-21 is a $CD4^+$T cell-derived cytokine that has a variety of biological functions, playing an immune regulatory role.[4–6] For example, IL-21 can enhance the activities of T and NK cells in an antitumor murine tumor model, and the combined use of IL-21 and granulocyte-macrophage colony-stimulating factor cytokines has resulted in prolonged tumor-bearing mouse survival.[5–8]

Increasing evidence shows that the mesenchymal stem cells (MSCs) are primitive cells, which have the effect of self-renewal and multi-differentiation, and thus represent a potential source for delivery of therapeutic agents to tumor tissues in cell-based therapy of cancers.[9,10] Since MSC posses the characteristic of immunoprivilege, they have been served as a useful targeted transmissive vector for a local production of biological agents to treat refractory diseases, which has raised wide interest in delivering genes specifically to tumors as a therapeutic mode.[11–14]

MiRNA (miR)-200c has emerged as potential therapeutic candidate by virtue of its capability to downregulate multiple targets involved in tumor progression, metastasis, therapeutic resistance, and relapse.[15] The down-regulated miR-200c expression has been found in ovarian cancer cell lines and in stage III ovarian tumors, but restoration of the miR-200c acts as a tumor suppressor by directly targeting the zinc-finger E-box binding homeobox 1 (ZEB1) and inhibiting the epithelial–mesenchymal transition (EMT) and metastasis of EOC.[15–17]

In view of the above-mentioned reports and the different biological functions of IL-21, the human umbilical cord MSCs (hUCMSCs), and miR-200c, we proposed a synergistic strategy that we used the lentivirus-carrying IL-21 gene to infect the hUCMSCs and to treat SKOV3 EOC in nude mouse model by injection of miR-200c agomir in this study, which may elicit the antitumor immune response (IL-21 action) and inhibit the EMT program (miR-200c action) concurrently to strengthen the fighting EOC efficacy. Our data showed that the anti-EOC efficacy mainly depended on the synthetic action of IL-21, hUCMSCs, and miR-200c via inhibition of Wnt/β-catenin signaling pathway and EMT of SKOV3 EOC.

Materials and methods

Cell lines and mice

The human EOC SKOV-3 cell line was purchased from the Cell Bank of the Chinese Academy of Sciences (Shanghai, China). Cells were maintained in complete media consisting of Roswell Park Memorial Institute (RPMI) 1640, 2 mM L-glutamine, 100 U/mL penicillin, 100 μg/mL streptomycin, and 10% fetal bovine serum (FBS). Human embryonic kidney (HEK) 293T cell line was also purchased from the Cellular Institute in Shanghai, China, and cultured in DMEM medium plus 10% FBS, 2 mmol/L L-glutamine, 100 u/mL penicillin, and 100 μg/mL streptomycin. All cells were cultured at 37°C in 5% CO_2 and complete media.

Balb/c athymic nu/nu mice were ordered from the Animal Center of Nang Jing University of China and were raised at the Experimental Animal Center, Southeast University. All the animal experiments were performed in compliance with the guidelines of the Animal Research Ethics Board of Southeast University. This ethics board also approved the animal studies.

Isolation and identification of hUCMSCs

All human umbilical cord blood samples were obtained from the Department of Gynecology & Obstetrics of Zhongda Hospital, Southeast University (Nanjing, Jiangsu, China). Our investigation was approved by the ethics committee at Southeast University School of Medicine, together with confirmation that informed consent was obtained from the donors for the use of the blood samples from the umbilical cords in pregnancy. The protocol was described in previous reports.[18,19]

Construction of lentiviral IL-21 recombinant and transduction of hUCMSCs

To generate the IL-21 expression lentivirus recombinant, we amplified IL-21 by PCR from template plasmid pRSC-IL-21 using the designed primers (sense: 5′-CATACTCGAGATG GAGAGGACCCTTGTCTGTCTGG-3′; antisense: 5′-GAC TGGATCCCTAGGAGAGATG CTGATGAATCATC-3). The lentivirus IL-21 and the lentiviral vector were produced from the transient transfection of the HEK293T cells with pHAGE-CMV-IL-21-IZsGreen, psPAX2, and pMD2. G plasmid DNAs plus Lipofectamine 2000 (Thermo Fisher Scientific, Waltham, MA, USA) according to the manufacturer's protocol. Forty-eight hours after the cotransfection, the lentivirus-bearing supernatants were collected and passed through a 0.45-mm filter. When hUCMSCs were 70% confluent in 6-well plate, cells were transduced with the pHAGE-CMV-IL-21-IzsGreen lentivirus, and were selected by the IzsGreen expression.[16]

Wound-healing assay

The experiment was divided into DMEM-F12 medium, hUCMSCs, hUCMSCs-LV-vector, hUCMSCs-LV-IL-21, miR-200c, hUCMSCs-LV-IL-21 combined with miR-200c, and cisplatin groups. The SKOV-3 cells were put in the upper chamber of the Transwell, and DMEM-F12 medium, hUCMSCs, hUCMSCs-LV-vector, hUCMSCs-LV-IL-21 were respectively put in the bottom chamber of the Transwell. In the hUCMSCs-LV-IL-21 combined with miR-200c group, SKOV-3 cells transfected with miR-200c mimic were put in the upper chamber, and hUCMSCs-LV-IL-21 were put in the bottom one; in the miR-200c group, SKOV-3 cells transfected with miR-200c mimic were put in the upper chamber, and DMEM-F12 medium were put in the bottom one; in the cisplatin group, SKOV-3 cells were put in the upper chamber, and 10 μg cisplatin/mL were put in the bottom one. After 24-h coculture, cells were grown to confluence and wounded by dragging a 1-mL pipette tip across their monolayer. Cells were washed to remove any cellular debris. Images were taken, using a DMI6000 inverted microscope (Leica Microsystems, Wetzlar, Germany), at 0, 24, and 72 h, respectively, after the wounding procedure.[20,21]

Invasion assay

The Transwell inserts with 8 μm pores were coated with Matrigel (20 μg/well; BD, Waltham, MA, USA) which was used for the invasion assay. Approximately, 10^4 cells treated with various agents were plated in the upper Transwell chamber and allowed to migrate to the lower chamber for 24 h. The Transwell membranes were then fixed and stained using Crystal Violet. The membranes were removed from the Transwell inserts and the cells on the undersurface of the Millipore membrane were counted under a light microscope (at an average of five semi-random non-overlapping fields at 200× magnification).[22]

Anti-ovarian cancer experiment in nude mice

A total of 42 Balb/c nude mice were randomly assigned to the above-mentioned seven groups (in vitro experiments) with every group containing six mice. Each group received subcutaneous inoculation of 5×10^6 SKOV3 cells at the mouse's right flank. About 8–9 days after the injection, tumors were visible to the naked eye. Then, 100 μL phosphate buffered saline (PBS), 1×10^6 different treated cells were injected into the mouse intratumoral sites. In the miR-200c group, miR-200c agomir (micrON™ miRNA agomir mouse mir-200c-3p; Bioribo Company, Guangzhou, China) in 0.1 mL saline buffer was locally injected nine times into the intratumoral sites once every 3 days.[16,23] In the cisplatin group, cisplatin (4 mg/kg) was locally injected into the intratumoral sites once every week; this was performed over 4 weeks. The tumor volumes were evaluated every 3 days by measuring two perpendicular diameters of the tumors using calipers.[24] All mice were sacrificed at 35 days after injection of different agents. In addition, five nude mice were used to observe the toxicity of hUCMSCs-LV-IL-21 combined with miR-200c analyzed by blood routine and renal function 60 days after injection.

ELISA for IFN-γ, IL-21, and TNF-α

The enzyme linked immunosorbent assay (ELISA) was performed to detect IFN-γ, IL-21, and TNF-α by following the kit's protocol (Thermo Fisher Scientific, Waltham, MA, USA). The kit is suitable for detecting samples that include cell culture supernatant and serum.[25]

Measurement of splenocyte cytotoxicity

The harvested splenocytes were used as the effector cells that were labeled with 0.5 mM 5-(and 6)-carboxy-fluorescein diacetate succinimidyl ester (CFSE; 20 μg/mL) at 37°C for 15 min. SKOV3 and YAC-1 cells were used as the target cells of the splenocytes and NK cells, respectively. The labeled splenocytes were washed twice in the PBS containing 5% FBS to sequester any free CFSE. The CFSE-labeled effector cells were seeded with a constant number of SKOV3 or YAC-1 target cells in a 96-well plate at the 25:1 ratios of the effector to the target cells. The cytotoxicity was analyzed with flow cytometry (FCM).[8,26]

Quantitative real-time reverse transcription-PCR (qPCR)

qPCR analysis was performed as described in our previous reports.[17,27] cDNAs were amplified by PCR with primers as follows: NKG2D (sense, 5′-TTTCTGCTGCTTCATCG ATGT-3′; antisense, 5′-TGATTTTGGAGGGATCTCGC-3′); MICA (sense, 5′-ACTAAGG AATGGACAATGCCC-3′; antisense, 5′-CACGGTAATGTTGCCCTCTGAG-3′); β-actin (sense, 5′-ACGGATTTGGTCGTATTGGG-3′; antisense, 5′-TGATTTTGGAGGGATCTC GC-3′). SYBR Green quantitative PCR amplifications were performed in the Step one plus Detection System (Thermo Fisher Scientific, Waltham, MA, USA). The comparative Ct (ΔΔCt) method was used to determine the expression fold change.

Western blotting

Approximately, 1×10^6 cells or tumor tissues were collected and lyzed in the protein extraction buffer (Novagen Inc., Madison, WI, USA) by following the manufacturer's protocol. The

membrane was then incubated with the goat anti-mouse IL-21, the rabbit anti-mouse/human ZEB1 (I-18; Santa Cruz Biotechnology Inc., Dallas, TX, USA), the rabbit anti-mouse/human β-catenin, cyclin-D1 E-cadherin, (Bioworld Technology Inc., MN, USA), and the rabbit anti-mouse/human Gli1/Gli2 antibody, (Abcam Inc., MA, USA), respectively, for overnight at 4°C. Immunoreactive bands were detected by Odyssey scanning instrument (Odyssey Imaging System; LI-COR Odyssey Imaging System, Nebraska, USA).[23,28]

Immunohistochemistry (IHC) and H&E staining

The tumor tissue sections from the tumor bearing mice were used to examine the expression of IL-21, β-catenin, cyclin-D1, E-cadherin, ZEB1 Gli1 and Gli2 by IHC.[29] The metastatic focus in the lung, liver, stomach, and spleen in the treated mice were analyzed with H&E staining as previous described.[11,19] The images were acquired by microscope TE2000-E (Nikon, Instech Co., Ltd., Tokyo, Japan), evaluated by two experienced pathologists and analyzed by Image pro-Plus6.0.

Statistical analysis

SPSS 17.0 and Graphpad Prism 5.0 were used for data analysis and imaging. Values of interest were presented as the mean ± standard deviation. Statistical analyses were performed using Student's *t*-test method and one-way analysis of variance (ANOVA) correction was used where multiple comparisons were made.[30]

Results

Combination of hUCMSCs-LV-IL-21 with miR-200c depresses SKOV3 cell mobility

To analyze the effect of the hUCMSCs-LV-IL-21 combined with miR-200c on SKOV3 cells, we examined the motility of SKOV3 cells with regard to cell migration and invasion abilities. The SKOV3 cells were treated with various agents as described in the "Materials and methods" section. The cell migration ability is displayed in Figure 1A. The hUCMSCs-LV-IL-21 combined with the miR-200c mimic clearly resulted in a significant reduction in cell migration compared

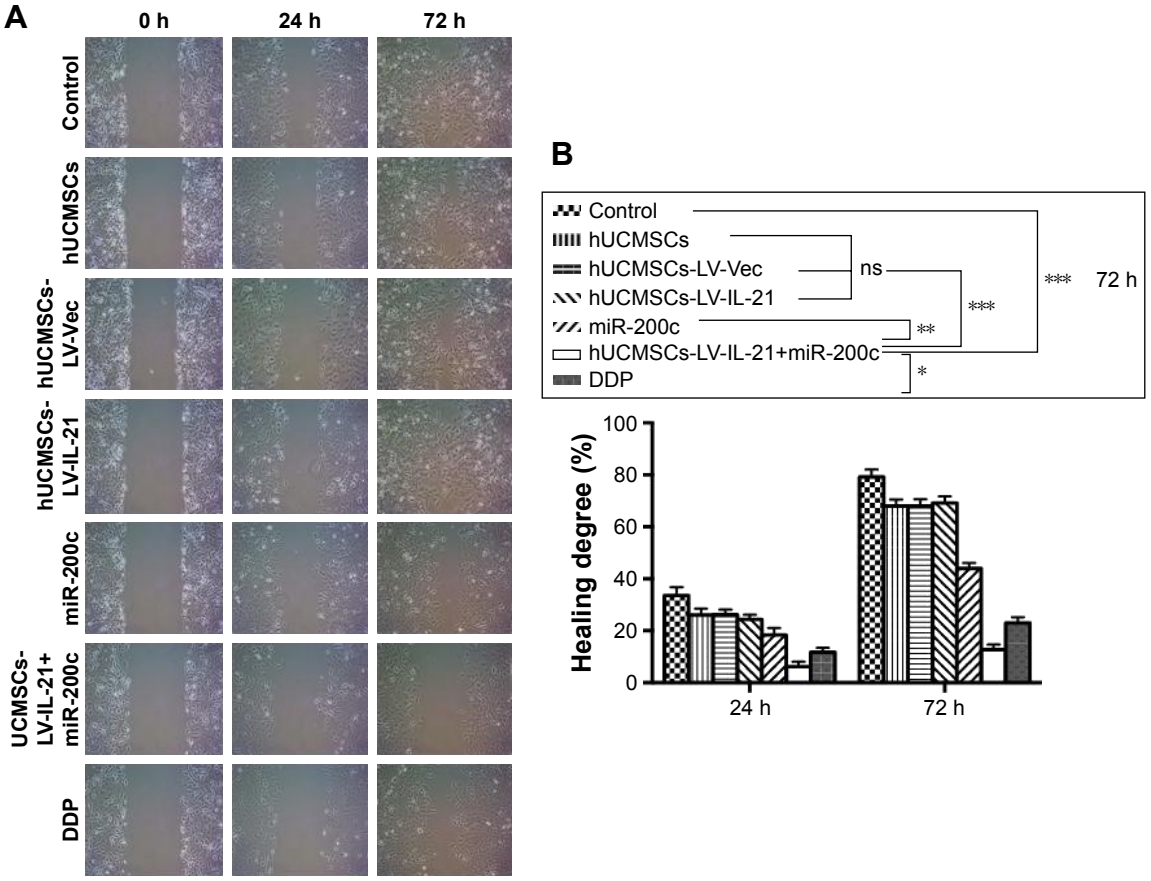

Figure 1 Analysis of the migration ability of SKOV3 cells treated with the different agents. (**A**) The migration ability of cells treated with the different agents detected by the wound healing assay. (**B**) The difference of cell healing degree percentage was statistically analyzed on 0 h, 24 h, and 72 h, respectively. *$p < 0.05$; **$p < 0.01$; ***$p < 0.005$.
Abbreviations: ns, no statistical significance; hUCMSCs, human umbilical cord mesenchymal stem cells.

with the control cells (hUCMSCs, hUCMSCs-LV-vector, miR-200c, hUCMSCs-LV-IL-21, and cisplatin-treated cells); the differences were statistically significant, as shown in Figure 1B. The cell invasion result indicated that the hUCMSCs-LV-IL-21 in combination with miR-200c-treated cells caused significantly fewer cells in the bottom of the chamber insert than those treated with hUCMSCs, hUCMSCs-LV-vector, miR-200c, hUCMSCs-LV-IL-21, and cisplatin (Figure 2A); the differences of statistical analyses are shown in Figure 2B. The results suggested that the SKOV3 cell motility was markedly inhibited when cells were treated with hUCMSCs-LV-IL-21 in combination with miR-200c in vitro.

hUCMSCs-LV-IL-21 combined with miR-200c against ovarian cancer growth and metastasis

Since the hUCMSCs-LV-IL-21 in combination with miR-200c in vitro exhibited significant inhibitive effect on the migration and invasion of SKOV3 cells, we sought to know whether the effect could affect the SKOV3 EOC progression in nude mouse model. The SKOV3 EOC growth curve diagram in Figure 3 was dynamically drawn from the differently treated mice when the tumor-bearing mice were euthanized on Day 35. It was found that the smallest tumor volume was in the mice treated with hUCMSCs-LV-IL-21 combined with miR-200c agomir among the seven groups. There were

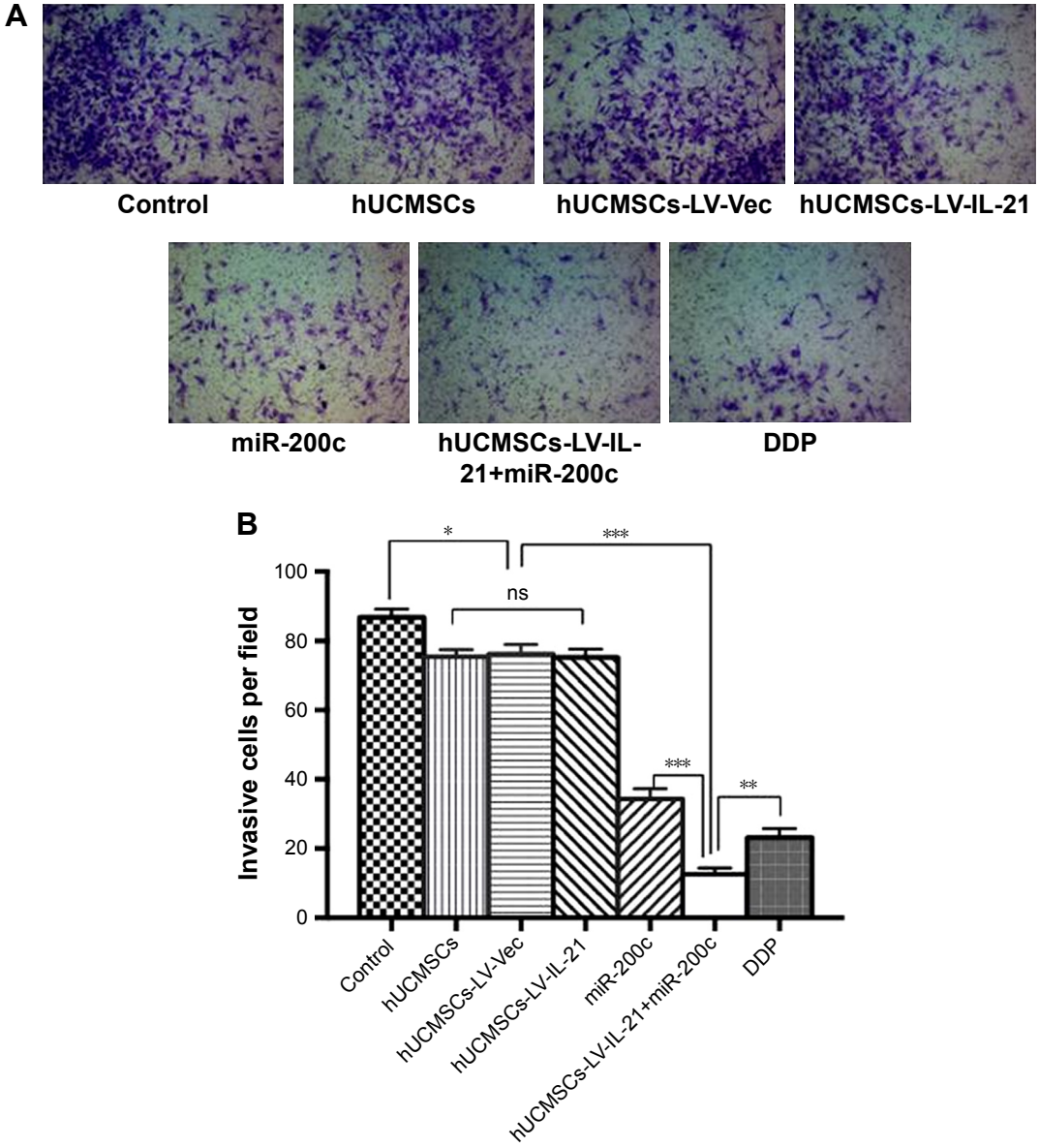

Figure 2 Analysis of the invasion ability of SKOV3 cells treated with the different agents. (**A**) The invasion ability of cells treated with the different agents was detected by the Transwell assay. (**B**) The difference of invasive cells per field was statistically analyzed on 24 h. *$p < 0.05$; **$p < 0.01$; ***$p < 0.005$.
Abbreviations: ns, no statistical significance; hUCMSCs, human umbilical cord mesenchymal stem cells.

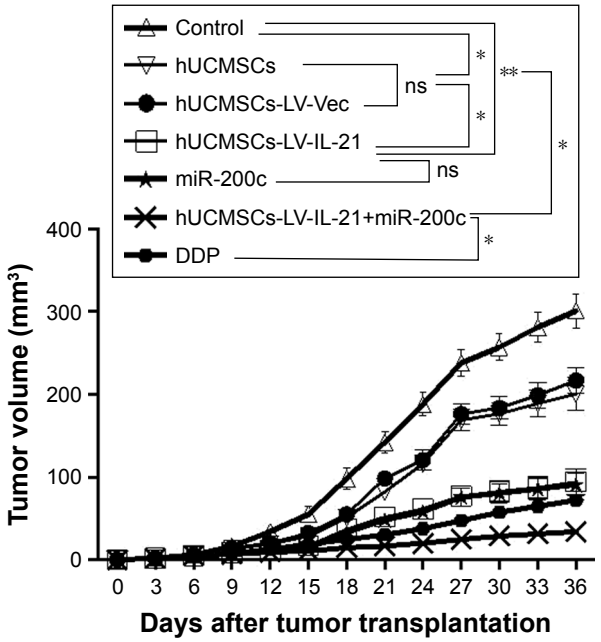

Figure 3 Combination therapy inhibits SKOV3 EOC growth in xenografted mice. The figure shows the quantification analysis of tumor volumes dynamically from the mice after they were initially injected s.c. with 5×10^6 SKOV3 cells followed by the treatment with a hUCMSCs-LV-IL-21+miR-200c, hUCMSCs-LV-IL-21, hUCMSCs, hUCMSCs-LV-Vec, miR-200c agomir, cisplatin (DDP), PBS, respectively. *$p < 0.05$ and **$p < 0.03$.
Abbreviations: ns, no statistical significance; EOC, epithelial ovarian cancer; s.c., subcutaneously; hUCMSCs, human umbilical cord mesenchymal stem cells.

significant differences between the hUCMSCs-LV-IL-21+ miR-200c agomir (combination) and hUCMSCs-LV-IL-21 groups ($p < 0.01$), between the combination and the miR-200c agomir groups ($p < 0.05$), and between the combination and the cisplatin groups ($p < 0.05$). Although the tumor volumes in the cisplatin group were smaller than that of miR-200c agomir group, no statistically significant difference was found between the two groups. The routine H&E staining showed there was no signs of ovarian cancer metastasis in lung, liver, stomach, and spleen in mice (data not shown). Additionally, there were no statistically significant toxic differences between the combination and any other control groups analyzed by blood routine and renal function (data not shown). The results from the animal experiments well demonstrated that the anti-EOC efficacy in the tumor bearing mice was found in the hUCMSCs-LV-IL-21 combined with miR200c group.

Immune responses induced by the different agents in tumor-bearing mice

The mouse immune responses induced by the different agents were evaluated. Because the cytotoxicity of splenocytes represents the anti-ovarian cancer efficacy in this study, we first analyzed the splenocyte cytotoxicity in the treated mice. As shown at the top of Figure 4A, the splenocyte cytotoxicity (splenocytes against SKOV3 target cells) in the hUCMSCs-LV-IL-21 group was the highest (76.14%) among the three treated groups; the hUCMSCs-LV-vector group ranked the second (51.66%), and the PBS group was the lowest (24.87%) among the three treated groups. The differences were statistically significant as shown in Figure 4B. The NK cytotoxic activity at the bottom of Figure 4A indicated that there were statistically significant differences ($p < 0.003$) between the hUCMSCs-LV-IL-21 and the PBS groups, and between the hUCMSCs-LV-IL-21 and the hUCMSCs-LV-vector groups ($p < 0.05$) as shown in Figure 4B. This was supported by the heightened expression of MIC A and NKG2D analyzed by qPCR (Figure 4C and D).

Subsequently, we investigated whether the serum cytokines IFN-γ, TNF-α, and IL-21 would be changed as well. Figure 5A shows that the IFN-γ level in the combination group was the highest among the seven treated groups. The difference was statistically significant between the combination and the miR-200c agomir groups ($p < 0.01$), between the combination and hUCMSCs-LV-vector groups ($p < 0.05$); but no statistically significant difference was found between the combination and the hUCMSCs-LV-IL-21 or the cisplatin groups. Similar cytokine TNF-α change was also found in mice treated with the different agents as shown in Figure 5B. As to IL-21 level, the hUCMSCs-LV-IL-21 group was the highest among the seven groups (Figure 5C). These results revealed that the hUCMSCs-LV-IL-21 combined with the miR200c to serve as a potential antitumor treatment against SKOV3 EOC by the induction of powerful immune responses in the treated mice.

Analysis of Wnt/β-catenin signaling and the EMT characteristic molecular expression

To understand the fighting SKOV3 EOC mechanisms of the hUCMSCs-LV-IL-21 in combination with the injection of the miR200c agomir, we analyzed the expression of Wnt/β-catenin signaling pathway and the EMT characteristic molecules, which are closely related to tumor cell growth and metastasis. Figure 6 (1–3, A, B) exhibits the expression of β-catenin, cyclin-D1, Gli1, Gli2, E-cadherin, ZEB1, and E-cadherin, respectively, in the tumor tissues from the different agent-treated mice, analyzed by the IHC. We found that the tumor cells from the mice treated with the combination agent significantly decreased the staining of β-catenin, cyclin-D1, Gli1, Gli2, and ZEB1, respectively, compared to those in the tumor cells from the mice treated with the any other agents. In contrast, the tumor cells notably increased the staining of E-cadherin in the combination agent-treated

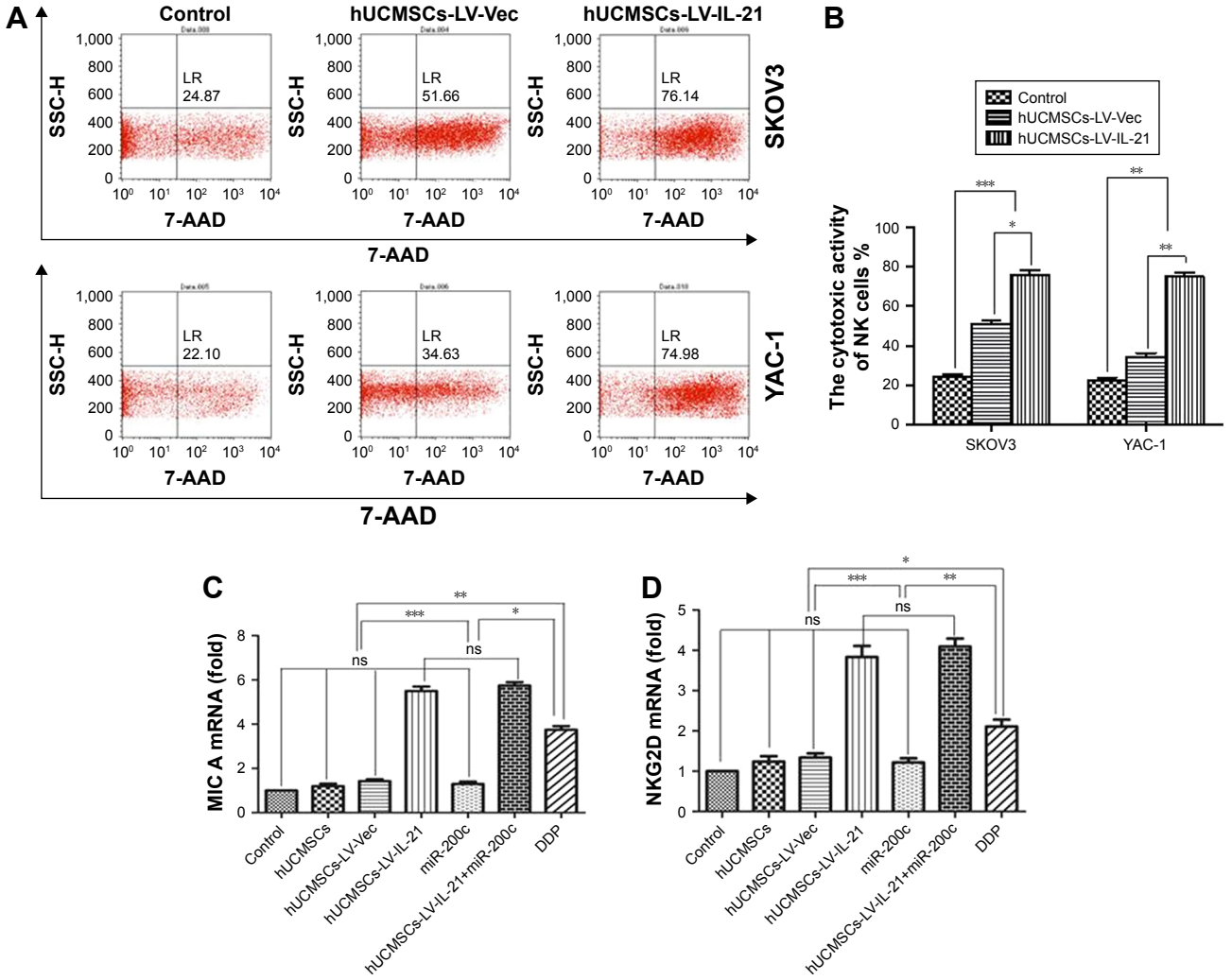

Figure 4 Treatment-associated responses of the splenocytes to target cells. (**A**) The splenocyte cytotoxicity (target cells: SKOV3, top) and NK cytotoxicity (target cells: YAC-1, bottom) were respectively analyzed by flow cytometry in the xenografted mice 35 days after the mice were initially injected s.c. with 5×10^6 SKOV3 cells followed by the treatment with various agents as described in the "Materials and methods" section. (**B**) Statistical analysis results of the splenocyte and NK cytotoxicities. (**C** and **D**) Quantification analysis of transcript expression of MIC A and NKG2D by qPCR. *$p < 0.05$, **$p < 0.03$, and ***$p < 0.003$.
Abbreviations: ns, no statistical significance; hUCMSCs, human umbilical cord mesenchymal stem cells; s.c., subcutaneously.

mice compared with any other agent-treated mice (Figure 6 [1–3, C and D]). These results were further supported by the data from the Western blot analysis. The bands of β-catenin, cyclin-D1, Gli1, Gli2, and ZEB1 were weaker in the samples of the mice that received the combination agent-treated group than those in the sample of mice that received any other agent-treated groups (Figure 7A and F); whereas the E-cadherin band was stronger in the combination agent-treated group than those in the samples of mice that received any other agent-treated groups, which were statistically significant as shown in Figure 7B–G and H. Taken together, these findings suggested that the hUCMSCs-LV-IL-21 combined with administration of miR200c agomir was able to inhibit the tumorigenesis and metastasis of SKOV3 cells in the nude mouse model.

Discussion

We had previously been able to develop the hUCMSCs-LV-IL-21 and had investigated the effect of hUCMSCs-LV-IL-21 as a vehicle for a constant source of transgenic IL-21 on ovarian cancer in vivo; however, the effect did not completely inhibit tumor growth.[19] In the present study, we used a novel agent of the hUCMSCs-LV-IL-21 combined with the miR200c to elicit immune responses against SKOV3 EOC and to inhibit tumor growth and metastases in a nude mouse model. We first demonstrated that the SKOV3 cells infected with the hUCMSCs-LV-IL-21 and miR200c mimic were markedly decreased in cell motility ability in vitro, and further demonstrated that the hUCMSCs-LV-IL-21 combined with the miR200c agomir injection significantly inhibited SKOV3 cell tumorigenicity in mice compared with any

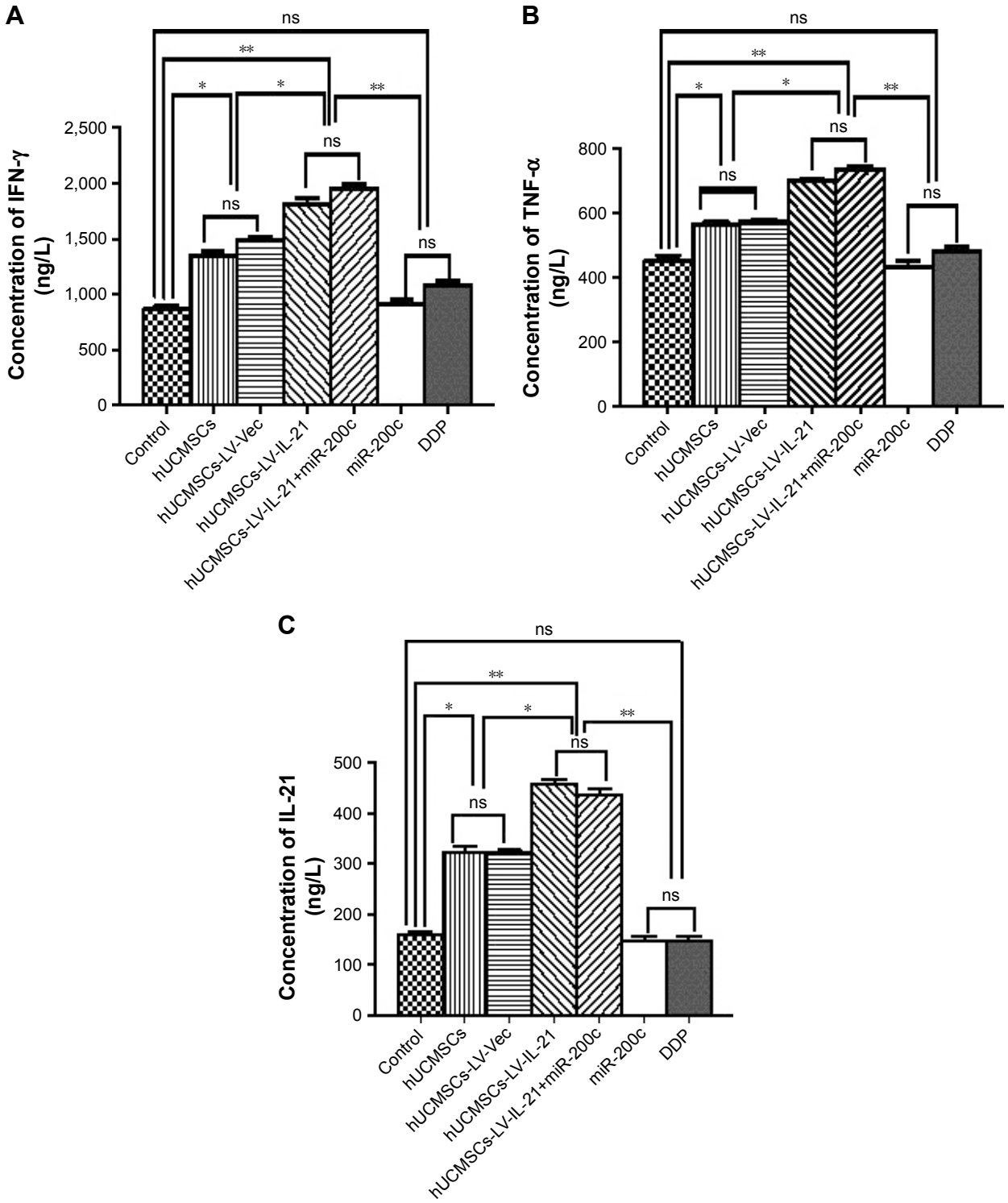

Figure 5 Serum levels of IFN-γ, IL-21, and TNF-α detected by ELISA. (**A**) Serum level of IFN-γ in the different groups. (**B**) Serum level of TNF-α in the different groups. (**C**) Serum level of IL-21 in the different groups. Data are represented as mean ± SEM (n = 6). *$p < 0.05$ and **$p < 0.03$.

Abbreviations: ELISA, enzyme linked immunosorbent assay; SEM, standard error of the mean; ns, no statistical significance; hUCMSCs, human umbilical cord mesenchymal stem cells.

other agents. In particular, miR-200c as a potential therapeutic candidate revealed an important role in anti-SKOV3 EOC. The results demonstrated well that this combination effectively decreased the tumor form in xenografted mice and prolonged the mouse survival.

Investigation of the molecular mechanisms revealed that the mice generated a significant splenocyte cytotoxicity to the SKOV3 or the YAC-1 cells induced by hUCMSCs-LV-IL-21. Meanwhile, the treated mice also showed an increase in the levels of IFN-γ, TNF-α, and IL-21. It has been reported

that these cytokines can react to NK cells and splenocytes, enhance their cytotoxic activities, and play a key biological role in killing tumor cells or inducing tumor cell apoptosis.[31,32] Our data demonstrated that high levels of IFN-γ, TNF-α, and IL-21 did strengthen the fighting SKOV3 EOC effectiveness and result in decreasing the SKOV3 xenograft growth and inhibiting metastatic focus in the lung, liver, stomach, and spleen in the mice that received hUCMSCs-LV-IL-21

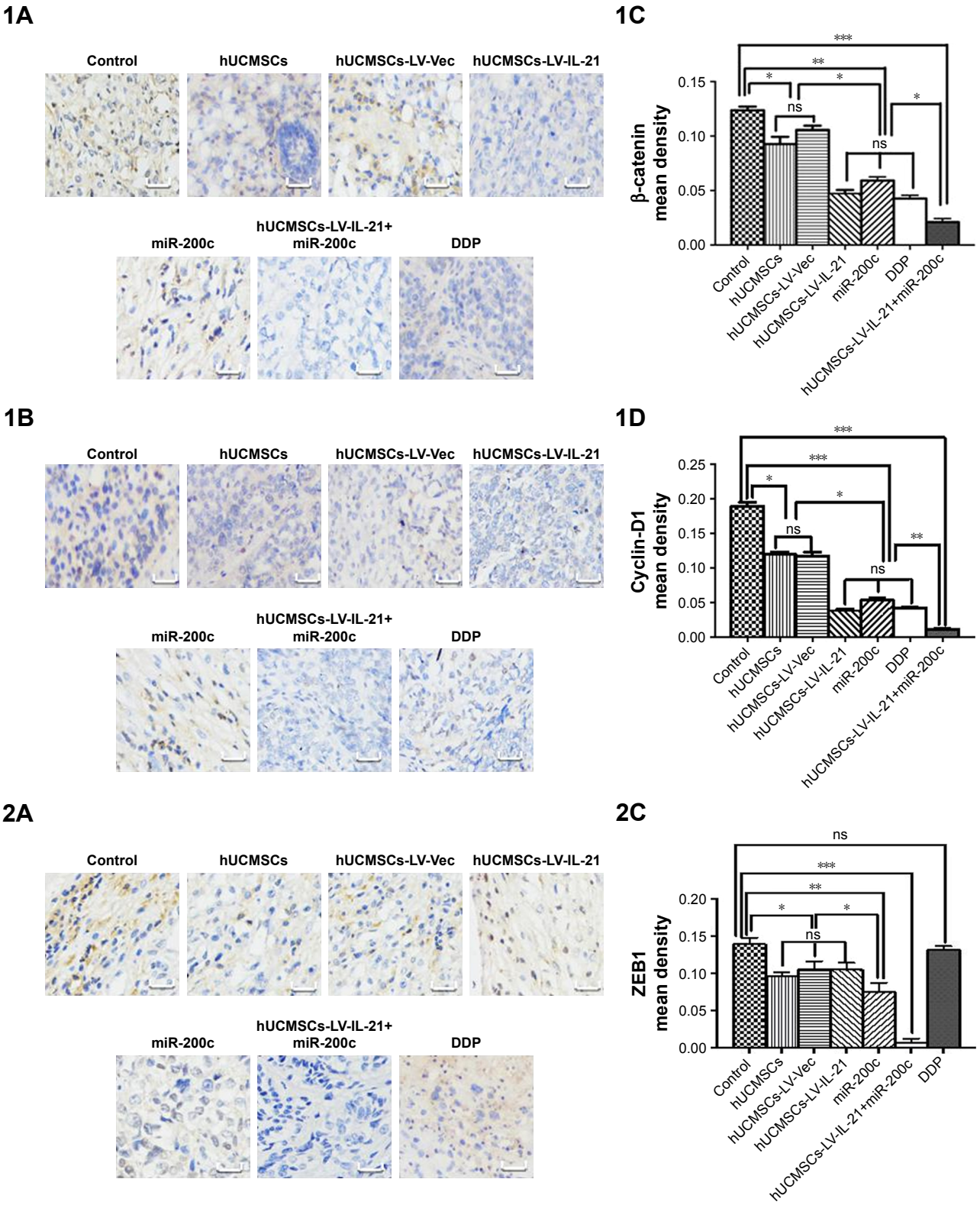

Figure 6 (*Continued*)

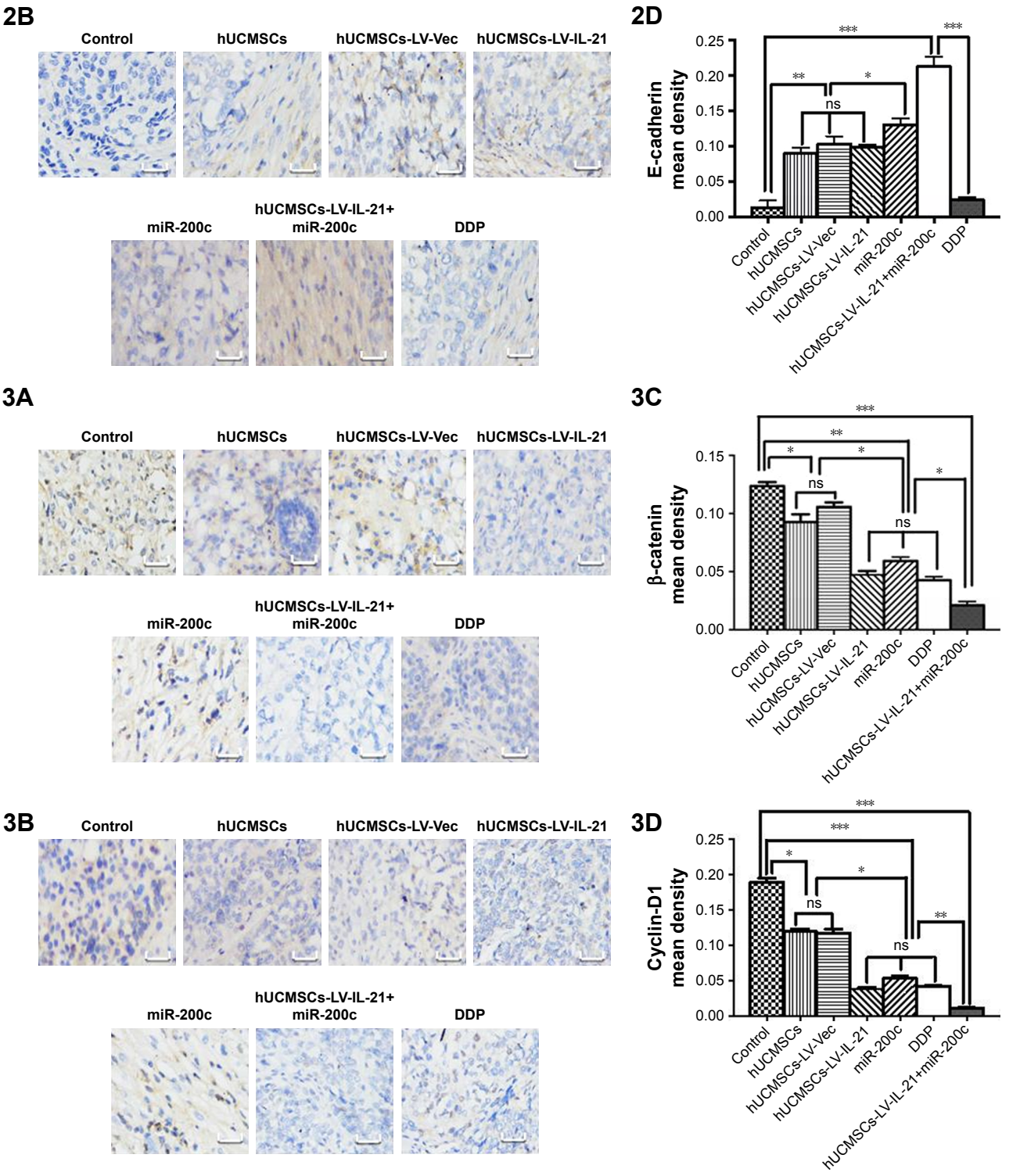

Figure 6 IHC analysis of Wnt/β-catenin signal pathway and EMT related-molecule expression in SKOV3 EOC tissues.
Notes: (1–3A, 1–3B) Images of Wnt/β-catenin signaling and EMT related-molecule expression of β-catenin, cyclin-D1, Gli1, Gli2, ZEB1, and E-cadherin in the tumor tissues analyzed with IHC (original magnification, ×400). **(1–3C, 1–3D)** The quantification analysis of the molecular expression. The brown color spots show the positive cells observed under a light microscopy. *$p < 0.05$, **$p < 0.03$, and ***$p < 0.003$.
Abbreviations: IHC, immunohistochemistry; EMT, epithelial–mesenchymal transition; ns, no statistical significance; hUCMSCs, human umbilical cord mesenchymal stem cells.

combined with the miR200c agomir administration. Additionally, the combination of treatment did not cause the toxicity to mice that manifested no renal function and blood routine abnormality (data not shown).

Works from our group[19,23,33,34] and others[35–37] have shown that the β-catenin is a pivotal component of the Wnt signaling pathway and it is closely regulated at the different levels of protein stability, subcellular localization, and transcriptional

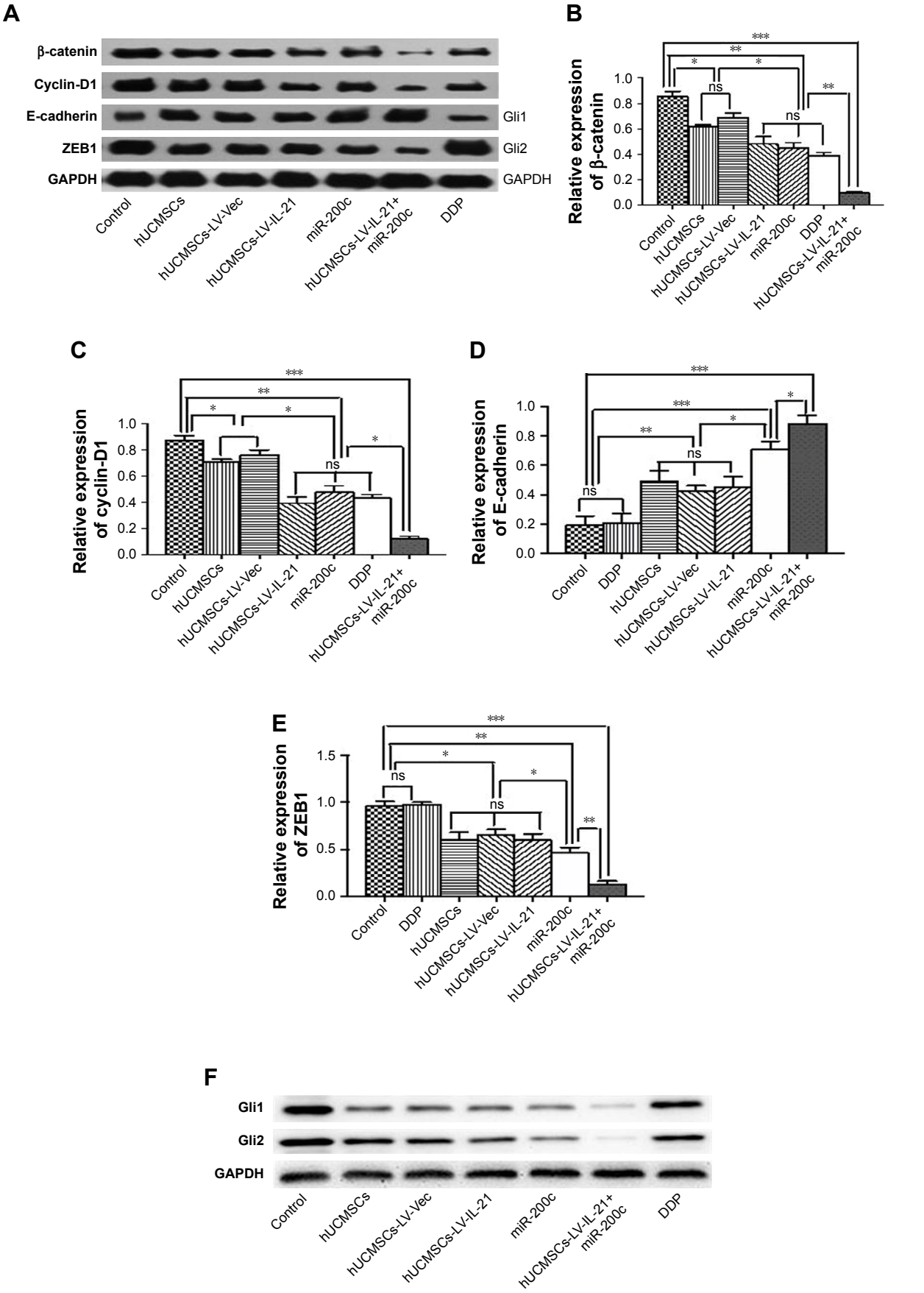

Figure 7 (*Continued*)

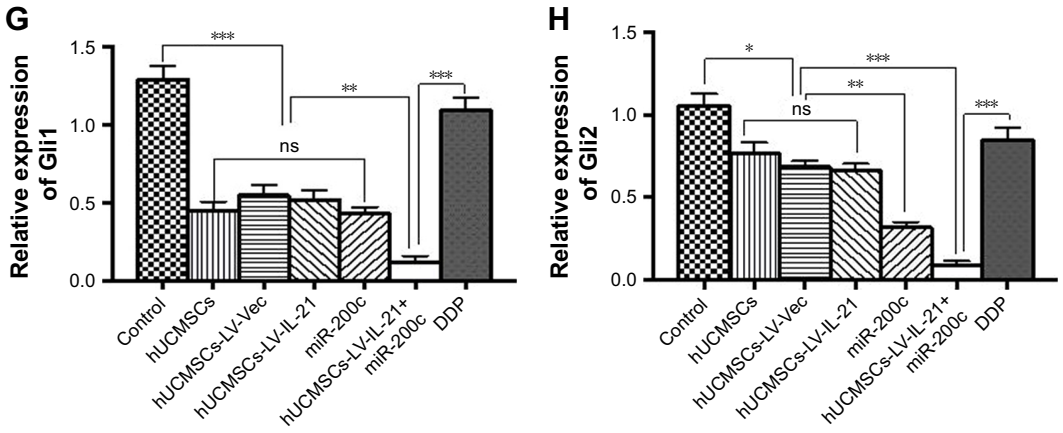

Figure 7 Western blot analysis of Wnt/β-catenin signal pathway and EMT related-molecule expression in SKOV3 EOC tissues. (**A** and **F**) The representative images of bands of the Wnt/β-catenin signaling and EMT related-molecule expression. (**B**–**E** and **G**–**H**) The semi-quantification analysis of the molecular expression. *$p < 0.05$, **$p < 0.03$, and ***$p < 0.003$.

Abbreviations: EMT, epithelial–mesenchymal transition; EOC, epithelial ovarian cancer; ns, no statistical significance; hUCMSCs, human umbilical cord mesenchymal stem cells.

activity. The Wnt/β-catenin signal pathway is an evolutionarily conserved and versatile pathway involving in embryonic development, tissue homeostasis, and various human diseases development. Aberrant activation of this pathway results in accumulating of β-catenin in the nucleus and accelerates the transcription of cyclin D-1 oncogene and EMT program, which may contribute to tumorigenesis and several cancer progression, including colon cancer, ovarian cancer, lung cancer, hepatocellular carcinoma, and pancreatic cancer.[35] The Gli2 transcription factor is known to be often overexpressed in cancers and contributes to the progression of a variety of neoplasms by regulating the cell cycle progression and apoptosis; the Gli1 protein is a direct target of Gli2 and could induce EMT in the kidney epithelial cells of rat via induction of snail, an epithelial cell marker E-cadherin repressor.[38,39] The ZEB1 also is a transcription factor that is essential for the physiological processes of differentiation, cell growth, and cell death; it is overexpressed in EOC and plays an important role in EOC invasion and metastasis by directly repressing the expression of the E-cadherin.[40] To this end, we analyzed the Wnt/β-catenin signaling pathway and EMT related-molecular expression in the tumor tissues. The data from the IHC and the Western blot assays showed statistically significant differences in decreased expression of β-catenin, cyclin-D1, Gli1, Gli2, and ZEB1 and in increased E-cadherin expression between the combination group and the other groups. We hypothesized that the change of the β-catenin and cyclin-D1 molecular expression decreased the ZEB1, Gli1, and Gli2 expression, which resulted in increasing the expression of E-cadherin in the SKOV3 xenografted tissues. Meanwhile, the heightened transcript expression of MIC A and NKG2D (Figure 4C and D) reinforced the NK cytotoxicity to the SKOV3 EOC. This comprehensive effect may lead to inhibition of tumor growth and the Wnt/β-catenin signaling pathway as well as EMT related-molecular expression.

Although the above-mentioned findings are encouraging, numerous questions remain unanswered. For example, the relevance of the NK activity and miR200c agomir in the immunotherapeutic combination, particularly in respect to their influence on fighting SKOV3 EOC efficacy, is worthy of further investigation.

Because the deregulated expression of the miR-200c has been detected in different EOC investigations, and the potential usefulness of the miR-200c serves as prognostic indicators in cancers, such as disease stage, tumor histology, survival and response to chemotherapy,[16,17,23,24,41] we believe the usefulness of the miR-200c combined hUCMSCs-LV-IL-21 may highlight the tendency that the clinical translational prospect of this drug combination will be feasible in EOC treatment.

Conclusion

Our data indicated that the administration of hUCMSCs-LV-IL-21 and miR200c agomir revealed the optimized synergism of antitumor regimen in the SKOV3 EOC-bearing mouse model. The findings well demonstrated that the inhibition of Wnt/β-catenin signal pathway and EMT of SKOV3 cells is a potential strategy for the treatment of SKOV3 EOC.

Acknowledgments

This work was supported in part by the National Natural Science Foundation of China (No. 81572887), and partly supported by the Funds for Outstanding PhD Academic Dissertations Candidate, Southeast University (YBJJ1746) as well as partly supported by the Collaborative Innovation

Center of Suzhou NanoScience and Technology. We also thank Dr Lin Wang in Educational Testing Service, USA, for checking and editing our manuscript.

Disclosure

The authors report no conflicts of interest in this work.

References

1. Ho CM, Chang SF, Hsiao CC, Chien TY, Shih DT. Isolation and characterization of stromal progenitor cells from ascites of patients with epithelial ovarian adenocarcinoma. *J Biomed Sci*. 2012;19:23.
2. Ayhan A, Gultekin M, Dursun P, et al. Metastatic lymph node number in epithelial ovarian carcinoma, does it have any clinical significance? *Gynecol Oncol*. 2008;108(2):428–432.
3. Meserve EEK, Mirkovic J, Conner JR, et al. Frequency of "incidental" serous tubal intraepithelial carcinoma (STIC) in women without a history of or genetic risk factor for high-grade serous carcinoma: A six-year study. *Gynecol Oncol*. 2017;146(1):69–73.
4. Parrish-Novak J, Dillon SR, Nelson A, et al. Interleukin 21 and its receptor are involved in NK cell expansion and regulation of lymphocyte function. *Nature*. 2000;408(6808):57–63.
5. Ugai S, Shimozato O, Kawamura K, et al. Expression of the interleukin-21 gene in murine colon carcinoma cells generates systemic immunity in the inoculated hosts. *Cancer Gene Ther*. 2003;10(10):771–778.
6. Dou J, Chen G, Wang J, et al. Preliminary study on mouse interleukin-21 application in tumor gene therapy. *Cell Mol Immunol*. 2004;1(6):461–466.
7. Venkatasubramanian S, Cheekatla S, Paidipally P, et al. IL-21-dependent expansion of memory-like NK cells enhances protective immune responses against Mycobacterium tuberculosis. *Mucosal Immunol*. 2017;10(4):1031–1042.
8. Zhao F, Dou J, Wang J, et al. Investigation on the anti-tumor efficacy by expression of GPI-anchored mIL-21 on the surface of B16F10 cells in C57BL/6 mice. *Immunobiology*. 2010;215(2):89–100.
9. Kim SM, Lim JY, Park SI, et al. Gene therapy using TRAIL-secreting human umbilical cord blood-derived mesenchymal stem cells against intracranial glioma. *Cancer Res*. 2008;68:9614–9623.
10. Alvarez-Mercado AI, Garcia-Mediavilla MV, Sanchez-Campos S, et al. Deleterious effect of human umbilical cord blood mononuclear cell transplantation on thioacetamide-induced chronic liver damage in rats. *Cell Transplant*. 2009;18(10):1069–1079.
11. Hu W, Wang J, Dou J, et al. Augmenting therapy of ovarian cancer efficacy by secreting IL-21 human umbilical cord blood stem cells in nude mice. *Cell Transplant*. 2011;20(5):669–680.
12. Bak XY, Lam DH, Yang J, et al. Human embryonic stem cell-derived mesenchymal stem cells as cellular delivery vehicles for prodrug gene therapy of glioblastoma. *Hum Gene Ther*. 2011;22(11):1365–1377.
13. Ryu CH, Park SH, Park SA, et al. Gene therapy of intracranial glioma using interleukin 12-secreting human umbilical cord blood-derived mesenchymal stem cells. *Hum Gene Ther*. 2011;22(6):733–743.
14. Chang YS, Oh W, Choi SJ, et al. Human umbilical cord blood-derived mesenchymal stem cells attenuate hyperoxia-induced lung injury in neonatal rats. *Cell Transplant*. 2009;18(8):869–886.
15. Bracken CP, Gregory PA, Kolesnikoff N, et al. A double-negative feedback loop between ZEB1-SIP1 and the microRNA-200 family regulates epithelial-mesenchymal transition. *Cancer Res*. 2008;68(19):7846–7854.
16. Cittelly DM, Dimitrova I, Howe EN, et al. Restoration of miR-200c to ovarian cancer reduces tumor burden and increases sensitivity to paclitaxel. *Mol Cancer Ther*. 2012;11(12):2556–2565.
17. Chen D, Zhang Y, Wang J, et al. MicroRNA-200c overexpression inhibits tumorigenicity and metastasis of $CD117^{+}CD44^{+}$ovarian cancer stem cells by regulating epithelial-mesenchymal transition. *J Ovarian Res*. 2013;6(1):50.
18. Wang HS, Hung SC, Peng ST, et al. Mesenchymal stem cells in the Wharton's jelly of the human umbilical cord. *Stem Cells*. 2004;22(7):1330–1337.
19. Zhang Y, Wang J, Ren M, et al. Gene therapy of ovarian cancer using IL-21-secreting human umbilical cord mesenchymal stem cells in nude mice. *J Ovarian Res*. 2014;7:8.
20. Dou J, Ni Y, He X, et al. Decreasing lncRNA HOTAIR expression inhibits human colorectal cancer stem cells. *Am J Transl Res*. 2016;8(1):98–108.
21. Shen B, Chu ES, Zhao G, et al. PPARgamma inhibits hepatocellular carcinoma metastases in vitro and in mice. *Br J Cancer*. 2012;106(9):1486–1494.
22. Marshall J. Transwell(®)invasion assays. *Methods Mol Biol*. 2011;769:97–110.
23. Wang X, Zhao F, He X, et al. Combining TGF-β1 knockdown and miR200c administration to optimize antitumor efficacy of B16F10/GPI-IL-21 vaccine. *Oncotarget*. 2015;6(14):12493–12504.
24. Dou J, He XF, Cao WH, et al. Overexpression of microRNA-200c in $CD44^{+}CD133^{+}$CSCS inhibits the cellular migratory and invasion as well as tumorigenicity in mice. *Cell Mol Biol (Noisy-le-grand)*. 2013;Suppl 59:OL1861–OL1868.
25. Rosenberg SA, Sherry RM, Morton KE, et al. Tumor progression can occur despite the induction of very high levels of self/tumor antigen-specific $CD8^{+}$T cells in patients with melanoma. *J Immunol*. 2005;175(9):6169–6176.
26. Lecoeur H, Février M, Garcia S, Rivière Y, Gougeon ML. A novel flow cytometric assay for quantitation and multiparametric characterization of cell-mediated cytotoxicity. *J Immunol Methods*. 2001;253(1–2):177–187.
27. Chen J, Wang J, Zhang Y, et al. Observation of ovarian cancer stem cell behavior and investigation of potential mechanisms of drug resistance in three-dimensional cell culture. *J Biosci Bioeng*. 2014;118(2):214–222.
28. Dou J, Liu P, Zhang X. Cellular response to gene expression profiles of different hepatitis C virus core protein in Huh-7 cell line with microarray analysis. *J Nanosci Nanotechnol*. 2005;5(8):1230–1235.
29. Shi SR, Liu C, Young L, Taylor C. Development of an optimal antigen retrieval protocol for immunohistochemistry of retinoblastoma protein (pRB) in formalin fixed, paraffin sections based on comparison of different methods. *Biotech Histochem*. 2007;82(6):301–309.
30. Hu W, Wang J, He X, et al. Human umbilical blood mononuclear cell-derived mesenchymal stem cells serve as interleukin-21 gene delivery vehicles for epithelial ovarian cancer therapy in nude mice. *Biotechnol Appl Biochem*. 2011;58(6):397–404.
31. Di Carlo E, Comes A, Orengo AM, et al. IL-21 induces tumor rejection by specific CTL and IFN-gamma-dependent *CXC* chemokines in syngeneic mice. *J Immunol*. 2004;172(3):1540–1547.
32. Dou J, Tang Q, Zhao F, et al. Comparison of immune responses induced in mice by vaccination with DNA vaccine constructs expressing mycobacterial antigen 85A and interleukin-21 and *Bacillus Galmette-Guérin*. *Immunol Invest*. 2008;37(2):113–127.
33. Wang J, Zhou D, He X, et al. Effect of downregulated β-catenin on cell proliferative activity, the sensitivity to chemotherapy drugs and tumorigenicity of ovarian cancer cells. *Cell Mol Biol (Noisy-le-grand)*. 2011;57 Suppl:OL1606–OL1613.
34. Dou J, He X, Liu Y, et al. Effect of downregulation of ZEB1 on vimentin expression, tumour migration and tumourigenicity of melanoma B16F10 cells and CSCs. *Cell Biol Int*. 2014;38(4):452–461.
35. Shang S, Hua F, Hu ZW. The regulation of β-catenin activity and function in cancer: therapeutic opportunities. *Oncotarget*. 2017;8(20):33972–33989.
36. Sun J, Yang X, Zhang R, et al. GOLPH3 induces epithelial-mesenchymal transition via Wnt/β-catenin signaling pathway in epithelial ovarian cancer. *Cancer Med*. 2017;6(4):834–844.
37. Li R, Dong T, Hu C, Lu J, Dai J, Liu P. Salinomycin repressed the epithelial-mesenchymal transition of epithelial ovarian cancer cells via downregulating Wnt/β-cateninpathway. *Onco Targets Ther*. 2017;10:1317–1325.

38. Ikram MS, Neill GW, Regl G, et al. GLI2 is expressed in normal human epidermis and BCC and induces GLI1 expression by binding to its promoter. *J Invest Dermatol*. 2004;122(6):1503–1509.
39. Dennler S, Andre J, Alexaki I, et al. Induction of sonic hedgehog mediators by transforming growth factor-beta: Smad3-dependent activation of Gli2 and Gli1 expression in vitro and in vivo. *Cancer Res*. 2007;67(14):6981–6986.
40. Thiery JP, Acloque H, Huang RY, Nieto MA. Epithelial-mesenchymal transitions in development and disease. *Cell*. 2009;139(5):871–890.
41. Koutsaki M, Libra M, Spandidos DA, Zaravinos A. The miR-200 family in ovarian cancer. *Oncotarget*. 2017;8(39):66629–66640.